Development and experimental validation of a numerical multibody model for the dynamic analysis of a counterbalance forklift truck

Leonardo Ventura[1], Giovanni Paolo Bonelli[2] and Alberto Martini[3]

[1] *School of Engineering and Materials Science, Queen Mary University of London, l.ventura@qmul.ac.uk*
[2] *Toyota Material Handling Manufacturing Italy SpA, giovanni.bonelli@toyota-industries.eu*
[3] *DIN – Dept. of Engineering for Industry, University of Bologna, alberto.martini6@unibo.it*

ABSTRACT — *This work investigates the dynamic behaviour of a prototypal counterbalance forklift truck. The final goal is implementing virtual testing tools to reliably assess the dynamic stresses acting on the specific forklift family of interest during a standard working cycle defined by the manufacturer's testing protocols. Indeed, unlike most of the other wheeled vehicles, forklifts typically do not have advanced suspension systems and their dynamic response is significantly affected by ground irregularities. Experimental tests are performed on the forklift to measure vibrations at six points of the vehicle when running on a speed bump at constant velocity, which is one of the most critical testing conditions. The experimental measurements are used for validating a rigid multibody model of the complete forklift. After model updating, a satisfactory agreement between numerical and experimental results is achieved.*

1 Introduction

Counterbalance forklift trucks are probably the most common type of material handling equipment in industrial applications. Typically, they do not have suspension systems with spring elements and/or shock absorbers to improve stability and provide isolation from the ground roughness, unlike most of the wheeled vehicles [1-3]. The vehicle is supported at three points (namely the two front wheels and the pivot point of the rear axle, which can freely swing) and tires constitute the most deformable components. Moreover, solid rubber tires or cushion tires are adopted for most applications, instead of pneumatic ones. Due to these specifications, the dynamic response of the vehicle can be significantly affected by small irregularities of the ground, like speed bumps and potholes. Indeed, impacts of the wheels on such obstacles during motion can cause instability and make the forklift tip over, thus representing a risk for safety [4]. In addition, the undamped energy of the impacts can generate transient overloads on the vehicle chassis and other components, hence inducing high vibration levels and durability issues [5].

The objective of this study is to investigate the dynamic behaviour of a prototypal heavy-duty forklift. The final goal of the manufacturer is implementing virtual testing tools to reliably assess the dynamic stresses acting on the specific family of counterbalance forklift trucks of interest during a standard working cycle defined by the manufacturer's testing protocols. Indeed, due to a combination of design features and relevant dynamic loads possibly experienced during operation, a careful evaluation of the actual strains/stresses affecting the chassis in working conditions is required.

As a first stage of the research, the focus is on developing and validating a numerical model to simulate the rigid body dynamics of the prototype for the case of passage over a speed bump, which is one of the most critical testing conditions in terms of dynamic stresses.

The paper is organized as follows. Section 2 describes the specifications of the studied forklift prototype. Section 3 reports the experimental tests. Section 4 describes the numerical model and the updating procedure. The final section draws the main conclusions of this study.

2 Overview of the studied forklift

The vehicle under investigation is a heavy-duty counterbalance forklift for both indoor and outdoor operation, referred to as model Traigo 80 by the manufacturer (Fig. 1). The main specifications of the studied configuration are reported in Tab. 1.

Two electric motors with planetary gearboxes (one for each side) independently drive the front wheels (namely, twin wheels with solid tires). Two wheels with identical tires are mounted at the rear (swinging) axle, which includes a hydraulic steering system. A further actuator with dedicated hydraulic circuit drives the mast and the forks. The cabin is mounted on conical elastomeric bearings.

The forklift features a highly asymmetric chassis, which is specifically conceived to permit automated fast replacement of the large battery (about 15% of the forklift mass). Because of this design, an accurate assessment of the actual strains/stresses characterizing the chassis in working conditions is essential.

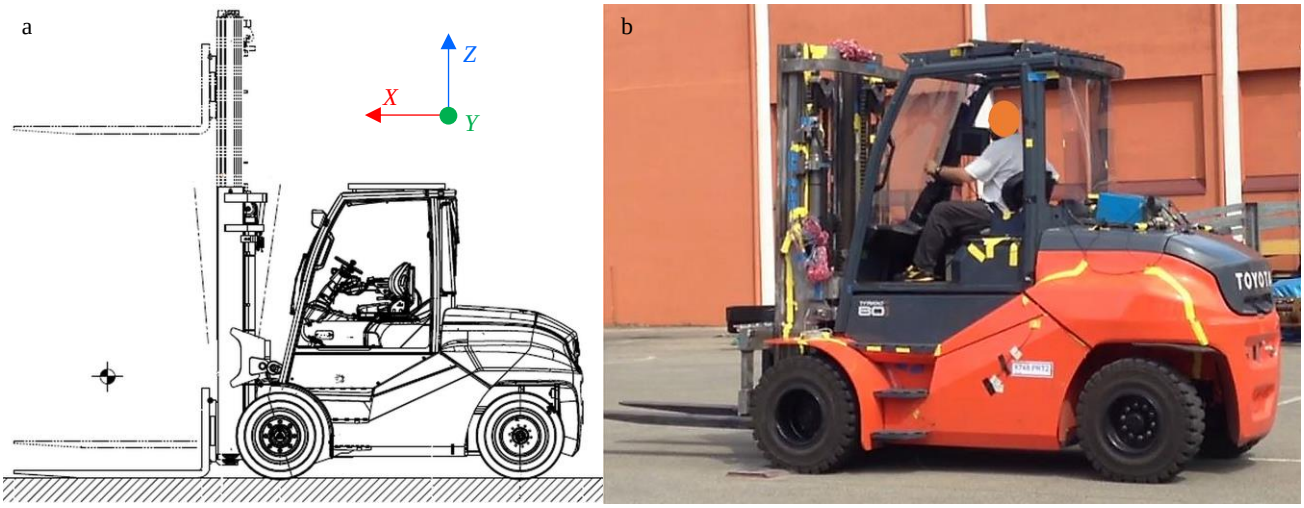

Fig. 1: (a) Schematics of the Traigo 80 forklift, (b) picture of the tested prototype

Feature	Value	Unit
Overall mass	15918	[kg]
front | rear mass distribution (unloaded)	7826 | 8092	[kg]
load capacity	8000	[kg]
battery mass	2785	[kg]
cabin mass	429	[kg]
Wheelbase	2300	[mm]
Lift height	3300	[mm]
Turning radius	3207	[mm]
Overall width	2141	[mm]

Tab. 1: Main specifications of the Traigo 80 forklift.

3 Experimental measurements

The experiments focus on a specific test condition, namely the unloaded forklift passing over an obstacle. Preliminary tests performed with different forklift configurations showed that such manoeuver can cause rebounds of the fork carriage, which can trigger the mast local modes and affect measurements, hence possibly hampering model validation.

The experiments presented and described in the following sections were perfomed with both the mast and the fork carriage constrained by belts in a fixed position, in order to avoid such unpredictable phenomena.

3.1 Sensor setup and tested conditions

Vibrations of the forklift are detected by means of six triaxial transducers, namely Dytran 7533A4 MEMS accelerometers (sensitivity 57 mV/g): one transducer is installed next to each wheel hub (Fig. 2); one sensor is mounted on the chassis, on the vehicle longitudinal centreline at about half the wheelbase; one accelerometer is placed in the cabin, under the operator's seat.

About twenty strain gauges (grid length 2 mm, resistance 120 Ω, uniaxial or 90°-biaxial, depending on the monitored location) are attached to the chassis for monitoring its deformations. Strain measurements will be adopted in the future steps of the research in order to validate flexible multibody models. Therefore, they will not be presented and discussed hereafter.

The measured signals are acquired by means of a VPG M-M System 7000 frontend, with a sampling frequency of 2 kHz and an additional digital low-pass filter (cutoff frequency of 400 Hz) applied to all the channels.

Experimental tests are performed by driving the unloaded forklift over a speed bump at a constant speed of 11 km/h. The obstacle, namely a steel block with trapezoidal cross-section (height 33 mm), is passed orthogonally, i.e. the front wheels climb over it simultaneously (Fig. 3). Fifteen runs are carried out in order to ensure repeatability.

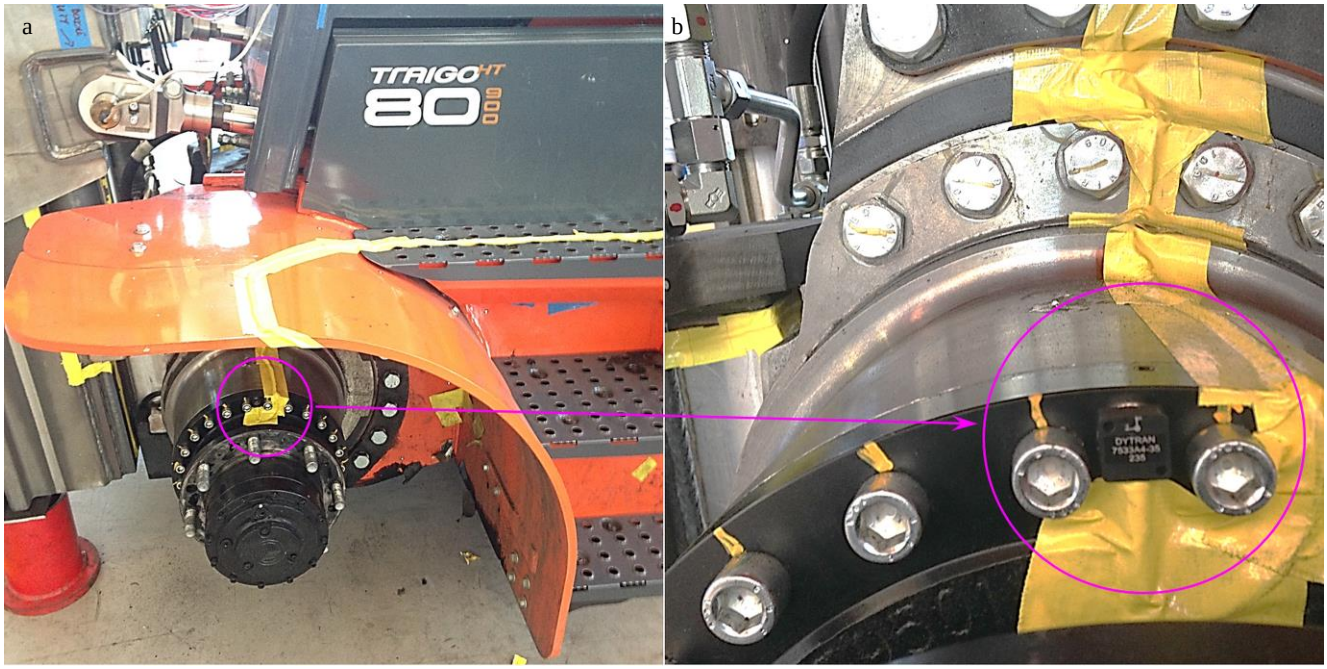

Fig. 2: (a) sensor setup on the hub of the left front wheel, (b) close up of the accelerometer.

Fig. 3: Close up of the steel obstacle during tests.

3.2 Experimental results

The measured signals exhibit a satisfactory repeatability, notwithstanding that the test conditions might have introduced some variability in the different runs (in particular, since a human operator drives the vehicle, its moving direction might have been not perfectly orthogonal to the obstacle). A lower standard deviation is observed for the sensors installed on the front wheel hubs: reasonably, the other signals are characterized by a greater variability due to the additional swinging Degree of Freedom (DOF) of the rear axle. In particular, the most consistent results are obtained for the vertical acceleration (i.e. along the z-axis) of the Front Left (FL) wheel hub. The comparison between the signals of all the fifteen runs (black curves) is shown in Fig. 4. Hence, the average vertical acceleration of the FL wheel hub (referred to as $\ddot{z}_{av}^{FL}$, also reported in Fig. 4 with a red line) is computed and adopted for model updating. The analysis focuses on such signal hereafter.

The $\ddot{z}_{av}^{FL}$ signal exhibits three main features: (i) a high peak (namely, the maximum acceleration value, referred to as $\ddot{z}_{av}^{FL}\{pk1\}$) can be observed when the front axle bounces over the obstacle (time 1.00 s); (ii) a second significant peak (at time 2.02 s, referred to as $\ddot{z}_{av}^{FL}\{pk2\}$) is generated by the interaction of the rear wheels with the obstacle; (iii) oscillations are present over the whole acquisition, their amplitude significantly growing when the first impact occurs.

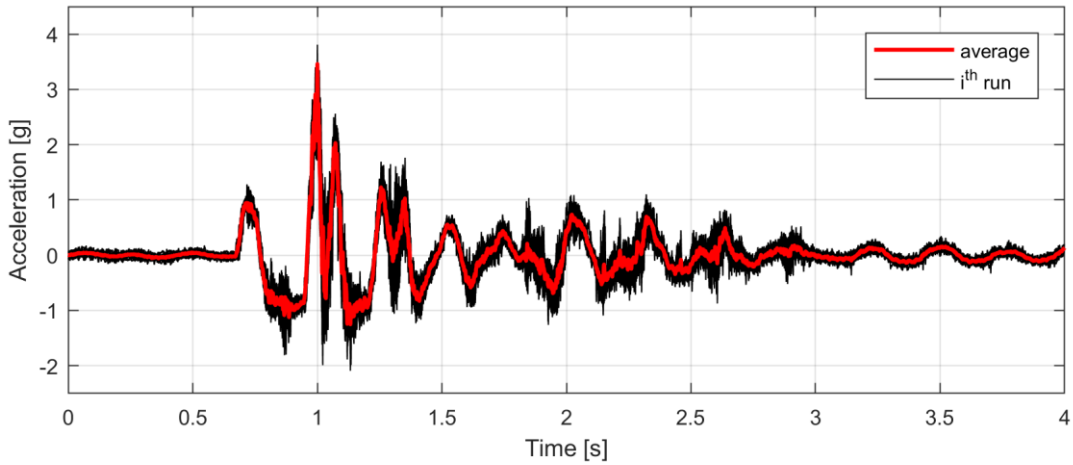

Fig. 4: FL wheel hub acceleration: comparison between the averaged signal, $\ddot{z}_{av}^{FL}$, and the 15 acquisitions.

The $\ddot{z}_{av}^{FL}$ signal is investigated in the frequency domain by computing Power Spectral Density (PSD). The analysis reveals two relevant spectral lines at about 3 and 3.8 Hz, respectively, while no significant frequency content is observed over 15 Hz (Fig. 5). In order to identify the vehicle mode shapes associated with the two most relevant frequency peaks, the phase differences of the vertical acceleration signals of all the wheels are assessed. In particular, the vertical accelerations are compared in the time domain after applying a band-pass filter (zero-phase FIR filter, centre frequency 3.5 Hz, bandwidth 2 Hz) [6]. The analysis shows that before the obstacle all the signals are in phase, hence the first resonance (i.e. the second highest peak in the PSD) being associated with the vehicle bounce mode. After the impact, the front accelerations are in phase, but in antiphase with the rear ones, thus the second resonance (which exhibits the highest amplitude in the spectrum), referred to as ω_{pE}, being related to the vehicle pitch mode.

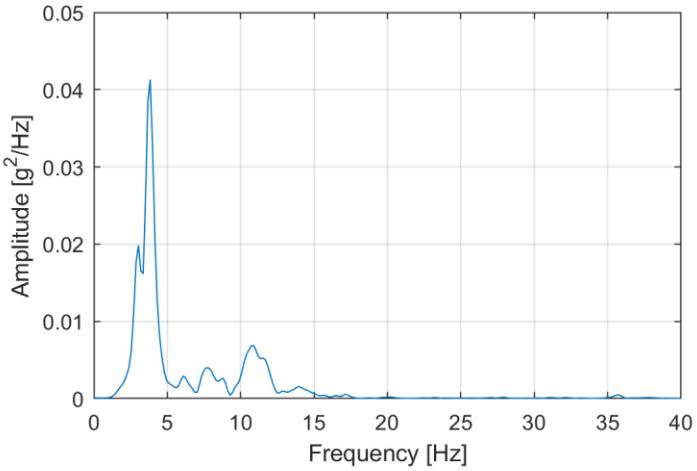

Fig. 5: PSD of the $\ddot{z}_{av}^{FL}$ signal.

4 Numerical model

4.1 Model implementation

A numerical model of the complete forklift truck is implemented by using a commercial multibody software, namely MSC Adams (Fig. 6). All the vehicle parts are modelled as rigid bodies. Their mass values are determined by means of direct measurements, whereas their inertia tensors are estimated through CAD models. The operator is considered as an additional non-deformable body of about 80 kg rigidly attached to the cabin.

Each wheel is connected to its hub by means of spring-damper elements (namely, three translational and two torsional elements) characterized by constant lumped parameters, to take into account the compliance of the joints, the mechanical transmission (front wheels) and the steering mechanism (rear wheels). Their stiffness values are estimated through static Finite Element analyses performed within Ansys Workbench environment.

Each cabin bearing is modelled by using three translational spring-damper elements. The corresponding stiffness and damping coefficients are determined according to the specifications found in the datasheet of the off-the-shelf components installed on the prototype.

As for the interactions between ground/obstacle and wheels, very few data can be found in the literature for solid rubber tires and at this stage of the research no specific experimental data characterizing the dynamic behaviour of the solid tires installed on the prototype were available. In light of this lack of information, the implementation of neither empirical tire models nor tailored analytical models appeared viable [7, 8]. Hence, contacts between tires and ground/obstacle are modelled with solid-to-solid impact functions. The contact stiffness is initialized by using the values inferred from the static load-deformation curve provided by the tire manufacturer. Friction (without stiction phenomena) is included in the contact model.

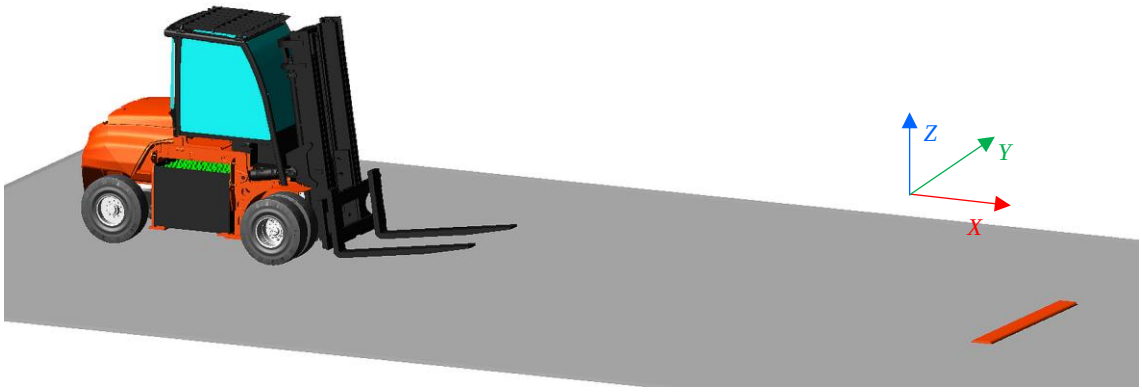

Fig. 6: Numerical model after static equilibrium solution.

All the other joints are modelled as ideal kinematic constraints.

Simulations are performed with a sequence of three steps. Firstly, static equilibrium of the forklift lying on the ground in steady state is solved. Secondly, the vehicle natural frequencies and vibration modes are determined through linearization of the system around its static equilibrium configuration. Finally, dynamic analysis is carried out by imposing motion on the driving wheels, as well as null steering angle on the rear wheels, thus replicating the experimental conditions. In particular, velocity cubic polynomial functions bringing the forklift from null velocity to a constant forward speed of 11 km/h are adopted.

The frequency of the pitch vibration mode (referred to as ω_{pS}) and the vertical acceleration of the front left wheel hub (referred to as $\ddot{z}_{sim}^{FL}$) are monitored for model updating purpose.

4.2 Model updating and validation

The numerical model is updated by using built-in optimization tools of multibody software. In particular, the design parameters (namely the unknowns of the optimization problem, i.e. the stiffness and damping parameters of both the tire contacts and the wheel bushings) are refined and the simulation sequence is repeated iteratively to minimize the following objective function:

$$obj\left(\mathbf{x}_{fr}\right)=\left|\ddot{z}_{av}^{FL}\left\{pk1\right\}-\ddot{z}_{sim}^{FL}\left\{pk1\right\}\right| \tag{1}$$

where $\mathbf{x}_{fr}$ is the vector of the unknowns for the forklift rigid-body model and $\ddot{z}_{sim}^{FL}\{pk1\}$ is the maximum acceleration peak associated with the passage of the front wheels on the obstacle, computed through the dynamic simulation. The following constraints must be satisfied:

$$\begin{cases}\mathbf{x}_{fr,min}\le\mathbf{x}_{fr}\le\mathbf{x}_{fr,max}\\ \left|\omega_{pE}-\omega_{pS}\right|\le 0.05\cdot\omega_{pE}\\ \left|\ddot{z}_{av}^{FL}\left\{pk2\right\}-\ddot{z}_{sim}^{FL}\left\{pk2\right\}\right|\le 0.1\cdot\ddot{z}_{av}^{FL}\left\{pk2\right\}\end{cases} \tag{2}$$

where $\mathbf{x}_{fr,min}$ and $\mathbf{x}_{fr,max}$ are the lower and upper bounds for the unknowns, respectively, and $\ddot{z}_{sim}^{FL}\{pk2\}$ is the positive acceleration peak related to the passage of the rear wheels on the obstacle.

After model updating, the simulation results show a satisfactory agreement with the experimental measurements. A comparison in the time domain between the measured and the simulated accelerations of the FL wheel hub is reported in Fig. 7.

Some discrepancies can be observed: higher-frequency vibrations are not properly caught by the model, in particular those associated with the impact of the front wheels; the initial phase of the impact (at about 0.75 [s])

is not accurately reproduced. Reasonably, the former issue may be solved by implementing flexible bodies, in particular a flexible chassis. As for the latter one, it is reasonably ascribable to an abrupt change in the direction of the contact force (caused by the geometry of the obstacle) and may be overcome by implementing a more refined contact model.

Nonetheless, the three features of interest, i.e. the two main acceleration peaks and the dominant vibration frequency, are matched with the desired accuracy. Hence, the rigid-body model is considered validated. Its main contact parameters are reported in Tab. 2. The updated model will be adopted as an effective starting point to develop a more complex flexible multibody model.

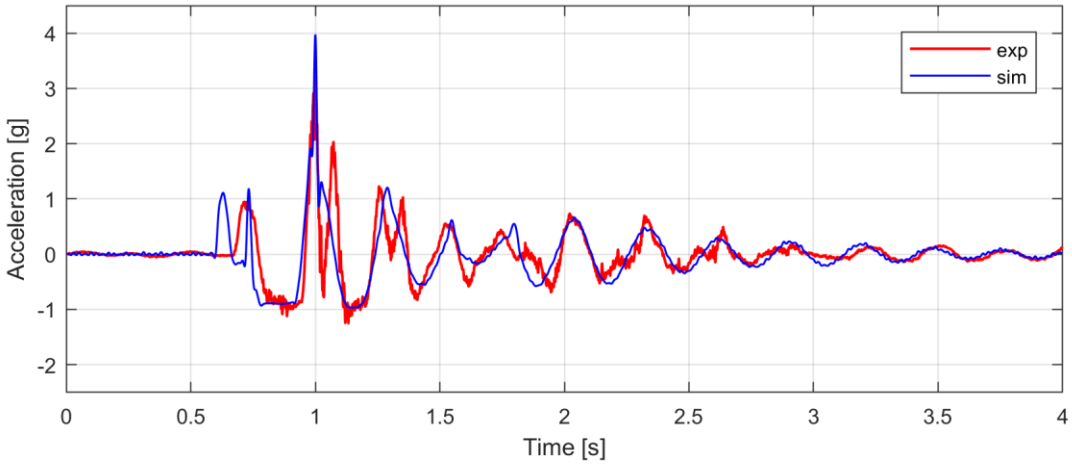

Fig. 7: Comparison between experimental data and numerical results: signals $\ddot{z}_{av}^{FL}$ (exp) and $\ddot{z}_{sim}^{FL}$ (sim).

Contact		Parameters				
		stiffness [N/m]	damping [N·s/m]	exponent	friction coefficient	
					static	dynamic
tire-road	front	$6.0 \cdot 10^6$	$5.0 \cdot 10^3$	1.5064	0.6	0.5
	rear	$6.0 \cdot 10^6$	$5.0 \cdot 10^3$	1.5064	0.6	0.5
tire-obstacle	front	$4.0 \cdot 10^6$	$7.5 \cdot 10^3$	1.5064	1.0	0.8
	rear	$7.2 \cdot 10^6$	$7.5 \cdot 10^3$	1.5064	1.0	0.8

Tab. 2: Main tire contact parameters of the Traigo 80 rigid-body model.

5 Conclusions

This study assessed the dynamic behaviour of a heavy-duty forklift prototype. A numerical rigid-body model was implemented to simulate one of the most critical conditions characterizing the manufacturer's test protocols for newly developed prototypes. The model was validated through experimental measurements.

The validated model provides a satisfactory estimation of the main characteristics of the vehicle dynamic response in the operating conditions of interest. It will be adopted as a starting point to develop a flexible multibody model to predict the dynamic stresses experienced by the forklift main structures when executing the prescribed test protocols. An improved model that includes flexible chassis is currently under development.

Acknowledgements

This activity is performed in collaboration with Toyota Material Handling Manufacturing Italy S.p.A. (Bologna,

Italy), that is gratefully acknowledged for operative cooperation, use of facilities, and financial support.

References

[1] D. Cao , X. Song and M. Ahmadian, "Editors' perspectives: road vehicle suspension design, dynamics, and control," *Vehicle System Dynamics*, vol. 49, no. 1-2, pp. 3 – 28, 2011.

[2] M. R. Azraai, G. Priyandoko, A. R. Yusoff and M. F. F. A. Rashid, "Parametric optimization of magneto-rheological fluid damper using particle swarm optimization," *International Journal of Automotive and Mechanical Engineering*, vol. 11, pp. 2591 – 2599, 2015.

[3] A. Martini and G. Bellani, "Numerical Investigation on the Dynamics of a High-Performance Motorcycle Equipped with an Innovative Hydro-Pneumatic Suspension System," in: *Proceedings of the 8th ECCOMAS Thematic Conference on Multibody Dynamics*, pp. 719–725, June 19 – 22, Prague, Czech Republic, 2017.

[4] J. Rebelle, P. Mistrot and R. Poirot, "Development and validation of a numerical model for predicting forklift truck tip-over," *Vehicle System Dynamics*, vol. 47, no. 7, pp. 771–804, 2009.

[5] M. Yang, G. Xu, Q. Dong and X. Han, "Vibration Study of Fork-lift Truck Based on the Virtual Prototype Technology," *Sensors & Transducers*, vol. 170, no. 5, pp. 177–183, 2014.

[6] A. Martini and M. Troncossi, "Upgrade of an automated line for plastic cap manufacture based on experimental vibration analysis," *Case Studies in Mechanical Systems and Signal Processing*, vol. 3, pp. 28-33, 2016. doi:10.1016/j.csmssp.2016.03.002

[7] H. B. Pacejka, *Tire and Vehicle Dynamics*. Oxford, UK: Butterworth-Heinemann, 3 ed., 2012.

[8] P. Lemerle and P. Mistrot, "A New Tire Model to Predict Vibration Emission of Counterbalance Trucks," *Tire Science and Technology*, vol. 28, no. 2, pp. 119-137, 2000. doi:10.2346/1.2135994